

Published in final edited form as:

*J Am Chem Soc.* 2011 February 2; 133(4): 676–679. doi:10.1021/ja108230s.

## Novel Pyrrolopyrimidine-Based $\alpha$ -Helix Mimetics: Cell-Permeable Inhibitors of Protein-Protein Interactions

Ji Hoon Lee<sup>†</sup>, Qi Zhang<sup>†</sup>, Sunhwan Jo<sup>‡</sup>, Sergio C. Chai<sup>†</sup>, Misook Oh<sup>†</sup>, Wonpil Im<sup>‡</sup>, Hua Lu<sup>\*,†</sup>, and Hyun-Suk Lim<sup>\*,†</sup>

<sup>†</sup>Department of Biochemistry and Molecular Biology, and Indiana University Simon Cancer Center, Indiana University School of Medicine, Indianapolis, Indiana 46202, United States

<sup>‡</sup>Department of Molecular Biosciences and Center for Bioinformatics, The University of Kansas, 2030 Becker Drive, Lawrence, Kansas 66047, United States

### Abstract

There is considerable interest in developing nonpeptidic, small molecule  $\alpha$ -helix mimetics to disrupt  $\alpha$ -helix-mediated protein-protein interactions. Herein, we report the design of a novel pyrrolopyrimidine-based scaffold for such  $\alpha$ -helix mimetics with increased conformational rigidity. We also developed a facile solid phase synthetic route, which is amenable to divergent synthesis of a large library. Using a fluorescence polarization-based assay, we identified cell permeable, dual MDMX/MDM2 inhibitors, demonstrating that the designed molecules can act as  $\alpha$ -helix mimetics.

$\alpha$ -Helices represent one of the most common protein secondary structures and are involved in various protein-protein interactions (PPIs). In many PPIs, short helical peptides play an important role as a recognition motif, where side chains at  $i$ ,  $i+3$  or  $i+4$ , and  $i+7$  positions often become a critical determinant for PPIs (Figure 1A).<sup>1</sup> Since  $\alpha$ -helix-mediated PPIs are involved in a wide array of cellular signaling pathways, inhibition of these interactions could be promising therapeutic targets. While peptide- and peptidomimetic-based approaches have shown successful applications to such targets,<sup>2</sup> non-peptidic, small molecules have advantages in terms of desirable bioavailability and cell permeability. Thus, there is considerable interest in developing non-peptidic, small molecule  $\alpha$ -helix mimetics that can disrupt such PPIs. Hamilton and co-workers demonstrated that rationally designed terphenyl **1** and similar scaffolds can serve as  $\alpha$ -helix mimetics (Figure 1B).<sup>1e</sup> Following their pioneering work, a number of terphenyl-inspired structures have been reported.<sup>1e-3</sup> While some of these compounds have been shown to effectively disrupt certain PPIs, there are several important issues associated with terphenyl-related structures, such as low aqueous solubility, relatively flexible scaffold structure, and long synthetic routes. Herein, we report design of a novel class of small molecule  $\alpha$ -helix mimetics, development of a facile solid-phase synthetic pathway, and a subsequent high-throughput screen, which led to the identification of potent inhibitors that disrupt the interaction between p53 and MDMX/MDM2.

On the basis of the Hamilton's terephthalamide **2** (Figure 1B),<sup>4</sup> we designed a pyrrolopyrimidine-based scaffold **3** (Figure 1C) with a hypothesis that the bicyclic ring in **3** could replace a pseudo-bicyclic structure formed by an intramolecular hydrogenbond in the terephthalamide **2**. Thus, the planar heterocyclic framework could provide a pre-organized

\* hualu@iupui.edu . \* limhyun@iupui.edu .

structure with increased conformational rigidity. An energy-minimization study suggests that three functional groups on R<sub>1</sub>, R<sub>2</sub>, and R<sub>3</sub> of this scaffold can mimic the spatial orientation of the side chains of *i*, *i*+3 or *i*+4, and *i*+7 amino acids in an  $\alpha$ -helix (Figure 1A,C). In addition, the pyrrolopyrimidine template is expected to possess favorable physical properties including water solubility and cell permeability, similar to its structurally related purine and indole scaffolds, which are frequently used as privileged scaffolds in biology and medicine.<sup>5</sup>

For the preparation of the designed compound **3**, we developed a straightforward solid-phase synthetic strategy by modifying a solution-phase synthesis of pyrrolopyrimidines (Scheme 1).<sup>6</sup> First, we utilized peptoid synthesis conditions to introduce two functionalities (R<sub>1</sub> and R<sub>2</sub>). This efficient sub-monomer route<sup>7</sup> includes bromoacetylation of amine group on Rink amide MBHA resin, followed by displacement of the bromide with primary amines. After repeating the same procedure, the resulting dimeric peptoids **6** were then coupled with 4,6-dichloro-2-(methylthio)pyrimidine-5-carbaldehyde to afford aldehydes **7** in nearly quantitative yield for 5 steps (Figure S1). Treatment of the aldehydes **7** with 1,8-diazabicyclo[5.4.0]undec-7-ene (DBU) in DMF and MeOH provided pyrrolopyrimidines **8** through concomitant cyclization and dimethylamination.<sup>8</sup> The thioether group was oxidized by *m*-chloroperbenzoic acid (mCPBA) to give a sulfone, which was subsequently substituted with various amines. The resin-bound tri-substituted bicyclic product **3** was cleaved with trifluoroacetic acid (TFA). Crude products were analyzed for purity and identity by LC-MS. To investigate efficiency of our synthetic pathway, a series of compounds **3** were synthesized employing a variety of different amines. Synthesis with most tested amines resulted in above 80% purity of the final products **3** as determined by LC-MS (Figure S1), which is sufficiently pure for biological testing without further purification. The most common by-product (< 5%) in the synthesis was 4-methoxy-substituted product (instead of the *N,N*-dimethylamino group) obtained during the cyclization step. Those amines that resulted in low purity (less than 70%) of final products were excluded in library synthesis. Compared to relatively lengthy, linear synthesis of most terphenyl-related structures, our synthetic route is simple and divergent and thus amenable to library synthesis. Notably, since many structurally diverse primary amines are commercially available, a large combinatorial library is readily accessible.

The efficacy of this scaffold as  $\alpha$ -helix mimetics was assessed by monitoring its ability to disrupt the p53-MDMX interaction. MDM2 and its homolog MDMX bind to the tumor suppressor p53 and regulate its stability and activity. The interactions are mediated mainly by three key residues (Phe19, Trp23, and Leu26) of p53 and the hydrophobic pocket in MDMX and MDM2 (Figure 2A).<sup>2a,2b</sup><sup>9</sup> Despite the similarity in the p53 recognition surface of MDMX and MDM2, it proved to be challenging to identify MDMX inhibitors, whereas a number of MDM2 inhibitors have been reported.<sup>10</sup> Indeed, inhibitors developed to target MDM2 show significantly less affinity to MDMX,<sup>9,11</sup> and there is only one report of MDMX-specific small molecule inhibitor.<sup>12</sup> Given that MDMX is overexpressed in many cancers and functions as a major regulator of p53 activity (both independently of and synergistically with MDM2), the development of MDMX inhibitors (either MDMX-specific or dual MDMX/MDM2 inhibitors) is highly desirable but still remains challenging.<sup>11,13</sup>

To search for such inhibitors, we constructed a 900-member library of compound **3** following Scheme 1. This was accomplished by a manual parallel synthesis (see Supporting Information for details). Primary amines containing hydrophobic groups (aromatic or aliphatic, shown in Figure S2) were selected with the intent of mimicking the side chains of the three amino acids of p53 (Phe, Trp, and Leu). For quality control, 90 compounds (10%) were randomly chosen from the library, and their purity and identity were verified by LC-MS. As shown in Table S1, the average purity of the crude final products was 83%,

indicating the robustness of the synthetic route. The library was used for screening without further purification. A computational modeling showed that the scaffold could mimic MDMX-bound p53 peptide (Figure 2B and Figure S3). The library molecules were screened at ~40  $\mu\text{M}$  concentration for the ability to displace a Rhodamine-labeled 15-mer p53 peptide from MDMX protein by a fluorescence polarization (FP) assay (Figure S4, See Supporting Information for details). From the screen, we identified two most active compounds, **3a** and **3b** (Figure 2C), which were resynthesized and purified by HPLC for further studies. The overall yields for the synthesis of **3a** and **3b** were 26% and 40%, respectively, based on the loading level of the resin (Figure S5). As expected, these compounds are highly soluble in aqueous solution.<sup>14,15</sup>

We assessed the binding affinities of the selected compounds using the same FP-based competitive assays. A 15-mer peptide derived from p53 and a known MDM2 inhibitor, MI-63,<sup>16</sup> were used as controls. As shown in Figure 3A, **3a** and **3b** effectively inhibited the p53-MDMX binding with  $K_i$  of 0.62  $\mu\text{M}$  and 0.45  $\mu\text{M}$ , respectively, which were comparable with that of a 15-mer p53 peptide ( $K_i = 0.8 \mu\text{M}$ ). We then tested whether they could bind to MDM2. Interestingly, they were found to inhibit the p53-MDM2 interaction as well with  $K_i$  of 0.62  $\mu\text{M}$  and 0.84  $\mu\text{M}$ , respectively, similar to the binding affinities for MDMX (Figure 3B,C). These results suggest that the compounds act as dual inhibitors of MDMX- and MDM2-p53 interactions.

Next we investigated the cellular activity of the inhibitors, since the compounds were expected to be cell permeable as indicated above. To test this, we examined the effect of the inhibitors on cellular levels of p53 and the cyclin-dependent kinase inhibitor p21, a major transcriptional target of p53. Human lung cancer H460 cells expressing wild type p53 were incubated with **3a**, **3b**, DMSO, or NC-1 (as a negative control), and cell lysates were analyzed by Western blot to monitor p53 and p21 levels. Indeed, treatment of **3a** and **3b** led to the increase of p53 and p21 levels in a dose-dependent manner, whereas DMSO and NC-1 had no effects (Figure 3D and Figure S6). This result clearly demonstrates that the compounds are not only cell-permeable, but also able to induce p53 level and activity in cells.

Activation of p53 by the MDMX/MDM2 inhibitors would result in cell cycle arrest and apoptosis. We examined the ability of the inhibitors to induce apoptosis by monitoring the effect of **3a** on caspase activity. H460 cells with wild type p53 and human lung cancer H1299 cells with deleted p53 were exposed to DMSO, NC-1, **3a**, or MI-63 (a positive control) for 24 hours, and caspase activity was measured by Caspase-Glo 3/7 assay kit (see Supporting Information). As shown in Figure 4, **3a** and MI-63 induced caspase 3/7 activity (about 3- and 5-fold, respectively) in H460 cells, while they had no effect on H1299 cells. This result indicates that **3a** triggers apoptosis through a p53-dependent pathway by binding to MDMX/MDM2 and inhibiting their function toward p53.

While unnatural oligomer-based dual MDMX/MDM2 inhibitors such as  $\beta$ -peptides<sup>17</sup> and N-acylpolyamines<sup>18</sup> have been reported, our compounds would have advantages as cell permeable, small 'drug-like' molecules. These dual-specific inhibitors should have a unique, but overlapping, mechanism with current MDM2 inhibitors and thus could provide a promising starting point for the development of a novel class of anti-cancer agents. Because the inhibitors are initial hit compounds, further studies are needed. These include biological evaluation of the inhibitors to elucidate the mode of mechanism as dual inhibitors, investigation of the selectivity of the compounds among  $\alpha$ -helix-recognizing proteins, and X-ray and computational studies to better understand the molecular basis for the binding. Experiments along these lines are underway.

In summary, we have described the design of a pyrrolopyrimidine-based scaffold **3** as a novel class of  $\alpha$ -helix mimetics and the development of a facile solid-phase synthetic route (Scheme 1). In addition, we have identified potent, dual inhibitors of MDMX- and MDM2-p53 interactions through high-throughput screening, highlighting that they can serve as  $\alpha$ -helix mimetics (Figure 2, 3 and 4). Of note, our compounds have several important advantages compared to most terphenyl-related structures, which include increased conformational rigidity, improved aqueous solubility, excellent cell permeability and ease of synthesis. Importantly, our divergent solid phase synthesis is amenable to the construction of large libraries and subsequent high-throughput screening. Taken together, we believe that our pyrrolopyrimidine-based scaffold along with the efficient solid phase synthesis will serve as a useful tool to discover inhibitors of many  $\alpha$ -helix-mediated PPIs.

## Supplementary Material

Refer to Web version on PubMed Central for supplementary material.

## Acknowledgments

We are grateful to Prof. Zhong-Yin Zhang (Indiana University) for critical reading of the manuscript, Prof. Qizhuang Ye (Indiana University) for providing access to a liquid handling system, and Dr. Jaeki Min (St. Jude Children's Research Hospital) for technical assistance. H. Lu was supported by NIH-NCI grants CA127724, CA095441, and CA129828. This research was also supported in part by NSF OCI-0503992 through TeraGrid resources provided by Purdue University.

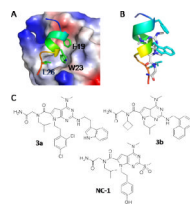
## REFERENCES

- (a) Davis JM, Tsou LK, Hamilton AD. *Chem. Soc. Rev.* 2007; 36:326. [PubMed: 17264933] (b) Hershberger SJ, Lee SG, Chmielewski J. *Curr. Top. Med. Chem.* 2007; 7:928. [PubMed: 17508924] (c) Wilson AJ. *Chem. Soc. Rev.* 2009; 38:3289. [PubMed: 20449049] (d) Jochim AL, Arora PS. *Mol. Biosyst.* 2009; 5:924. [PubMed: 19668855] (e) Cummings CG, Hamilton AD. *Curr. Opin. Chem. Biol.* 2010; 14:341. [PubMed: 20430687]
- (a) Pazgier M, Liu M, Zou G, Yuan W, Li C, Li C, Li J, Monbo J, Zella D, Tarasov SG, Lu W. *Proc. Natl. Acad. Sci. USA.* 2009; 106:4665. [PubMed: 19255450] (b) Phan J, Li Z, Kasprzak A, Li B, Sebti S, Guida W, Schönbrunn E, Chen J. *J. Biol. Chem.* 2010; 285:2174. [PubMed: 19910468] (c) Walensky LD, Kung AL, Escher I, Malia TJ, Barbuto S, Wright RD, Wagner G, Verdine GL, Korsmeyer SJ. *Science.* 2004; 305:1466. [PubMed: 15353804] (d) Fasan R, Dias RL, Moehle K, Zerbe O, Vrijbloed JW, Obrecht D, Robinson JA. *Angew. Chem. Int. Ed.* 2004; 43:2109. (e) Wang D, Liao W, Arora PS. *Angew. Chem. Int. Ed.* 2005; 44:6525. (f) Hara T, Durell SR, Myers MC, Appella DH. *J. Am. Chem. Soc.* 2006; 128:1995. [PubMed: 16464101] (g) Sadowsky JD, Fairlie WD, Hadley EB, Lee HS, Umezawa N, Nikolovska-Coleska Z, Wang S, Huang DC, Tomita Y, Gellman SH. *J. Am. Chem. Soc.* 2007; 129:139. [PubMed: 17199293] (h) Bautista AD, Appelbaum JS, Craig CJ, Michel J, Schepartz A. *J. Am. Chem. Soc.* 2010; 132:2904. [PubMed: 20158215]
- (a) Lu F, Chi SW, Kim DH, Han KH, Kuntz ID, Guy RK. *J. Comb. Chem.* 2006; 8:315. [PubMed: 16677000] (b) Volonterio A, Moisan L, Rebek J Jr. *Org. Lett.* 2007; 9:3733. [PubMed: 17711290] (c) Maity P, Konig B. *Org. Lett.* 2008; 10:1473. [PubMed: 18335950] (d) Plante JP, Burnley T, Malkova B, Webb ME, Warriner SL, Edwards TA, Wilson AJ. *Chem. Commun.* 2009:5091. (e) Shaginian A, Whitby LR, Hong S, Hwang I, Farooqi B, Searcey M, Chen J, Vogt PK, Boger D. *J. Am. Chem. Soc.* 2009; 131:5564. [PubMed: 19334711] (f) Marimganti S, Cheemala MN, Ahn J-M. *Org. Lett.* 2009; 11:4418. [PubMed: 19719090] (g) Tosovska P, Arora PS. *Org. Lett.* 2010; 12:1588. [PubMed: 20196543] (h) Bourne GT, Kuster DJ, Marshall GR. *Chemistry.* 2010; 16:8439. [PubMed: 20564292]
- Yin H, Lee GI, Sedey KA, Rodriguez JM, Wang HG, Sebti SM, Hamilton AD. *J. Am. Chem. Soc.* 2005; 127:5463. [PubMed: 15826183]
- Welsch ME, Snyder SA, Stockwell BR. *Curr. Opin. Chem. Biol.* 2010; 14:347. [PubMed: 20303320]
- Clark MP, et al. *Bioorg. Med. Chem. Lett.* 2007; 17:1250. [PubMed: 17189692]

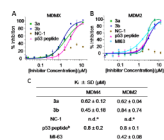
7. Figliozzi GM, Goldsmith R, Ng SC, Banville SC, Zuckermann RN. *Methods Enzymol.* 1996; 267:437. [PubMed: 8743331]
8. Agarwal A, Chauhan PMS. *Syn. Commun.* 2004; 34:2925.
9. Czarna A, Popowicz GM, Pecak A, Wolf S, Dubin G, Holak TA. *Cell Cycle.* 2009; 8:1176. [PubMed: 19305137]
10. (a) Murray JK, Gellman SH. *Biopolymers.* 2007; 88:657. [PubMed: 17427181] (b) Dömling A. *Curr. Opin. Chem. Biol.* 2008; 12:281. [PubMed: 18501203] (c) Shangary S, Wang S. *Annu. Rev. Pharmacol. Toxicol.* 2009; 49:223. [PubMed: 18834305]
11. Laurie NA, et al. *Nature.* 2006; 444:61. [PubMed: 17080083]
12. Reed D, Shen Y, Shelat AA, Arnold LA, Ferreira AM, Zhu F, Mills N, Smithson DC, Regni CA, Bashford D, Cicero SA, Schulman BA, Jochemsen AG, Guy RK, Dyer MA. *J. Biol. Chem.* 2010; 285:10786. [PubMed: 20080970]
13. (a) Toledo F, Wahl GM. *Nat. Rev. Cancer.* 2006; 6:909. [PubMed: 17128209] (b) Marine JC, Dyer MA, Jochemsen AG. *J. Cell Sci.* 2006; 120:371. [PubMed: 17251377]
14. Solubility of **3a** and **3b** in water and phosphate buffer saline (pH 7.4) were >150  $\mu$ /ml, which is above desirable water solubility (100  $\mu$ /ml) for favorable oral absorption of drugs.15
15. Muller CE. *Chem. Biodiv.* 2009; 6:2071.
16. Ding K, Lu Y, Nikolovska-Coleska Z, Wang G, Qiu S, Shangary S, Gao W, Qin D, Stuckey J, Krajewski K, Roller PP, Wang S. *J. Med. Chem.* 2006; 49:3432. [PubMed: 16759082]
17. Michel J, Harker EA, Tirado-Rives J, Jorgensen WL, Schepartz A. *J. Am. Chem. Soc.* 2009; 131:6356. [PubMed: 19415930]
18. Hayashi R, Wang D, Hara T, Iera JA, Durell SR, Appella DH. *Bioorg. Med. Chem.* 2009; 17:7884. [PubMed: 19880322]



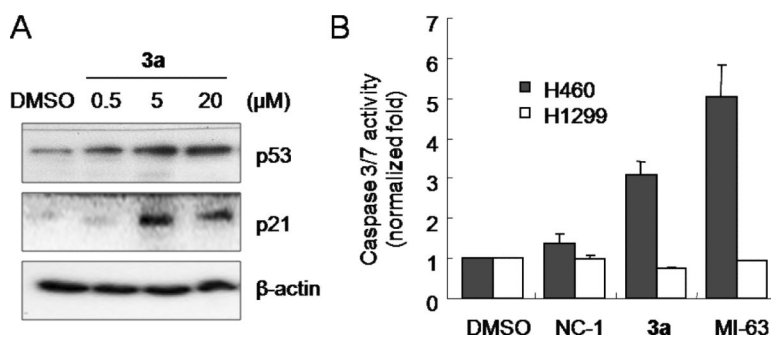
**Figure 1.** (A)  $\alpha$ -Helix with  $i$ ,  $i+4$ , and  $i+7$  side chain positions. (B)  $\alpha$ -Helix mimetics with terphenyl **1** and terephthalamide **2** scaffolds. (C) Pyrrolopyrimidine-based scaffold **3** and its energy-minimized conformation ( $R_1, R_2, R_3 = CH_3$ ).



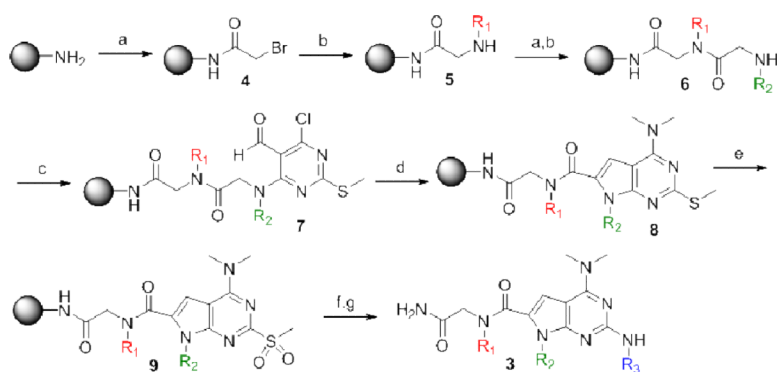
**Figure 2.** (A) Crystal structure of MDMX in complex with a p53 peptide (PDB entry: 2Z5S). (B) Overlay of compound **3** ( $R_1, R_2, R_3 = \text{CH}_3$ ) and an MDMX-bound p53 peptide. (C) Structures of the active compounds (**3a** and **3b**) and an inactive compound (NC-1).



**Figure 3.** Inhibition curves for Rhodamine-labeled p53 peptide (SQETFSDLWKLLPEN-NH-Rhodamine) binding to human MDMX (amino acids 1–137) (A) and human MDM2 (amino acids 1–138) (B) by fluorescence polarization. (C)  $K_i$  values of inhibitors. <sup>a</sup>Not determined. <sup>b</sup>Unlabeled 15-mer p53 peptide (SQETFSDLWKLLPEN).



**Figure 4.** p53 activation by **3a**. (A) Human lung cancer H460 cells expressing wild type p53 were treated with DMSO or the indicated concentrations of **3a** for 12 h. Lysates were subjected to Western blot analysis. (B) H460 cells with wild type p53 and human lung cancer H1299 cells with deleted p53 were exposed to DMSO, NC-1 (20  $\mu$ M), **3a** (20  $\mu$ M) or MI-63 (20  $\mu$ M) for 24 h. Caspase activity was analyzed by Caspase-Glo 3/7 assay kit (Promega).

**Scheme 1.**Solid-phase synthesis.<sup>a</sup>

<sup>a</sup>Reagents and conditions: (a) BrCH<sub>2</sub>CO<sub>2</sub>H, DIC, DMF, rt; (b) RNH<sub>2</sub>, DMF, rt; (c) 4,6-dichloro-2-(methylthio)pyrimidine-5-carbaldehyde, DIEA/DMF, rt; (d) DBU/DMF-MeOH, 90°C; (e) mCPBA, NaHCO<sub>3</sub>, DCM, rt; (f) R<sub>3</sub>NH<sub>2</sub>, DIEA/NMP, 170°C; (g) TFA/DCM, rt.